No.98 **Apr. 2022**

ISSN 0917-2211

Variable Star Bulletin

Romanov V48: unusual intermediate polar in the period gap

Taichi Kato[1],

tkato@kusastro.kyoto-u.ac.jp

Filipp D. Romanov[2]

filipp.romanov.27.04.1997@gmail.com, https://orcid.org/0000-0002-5268-7735

[1] Department of Astronomy, Kyoto University, Sakyo-ku, Kyoto 606-8502, Japan

[2] Pobedy street, house 7, flat 60, Yuzhno-Morskoy, Nakhodka, Primorsky Krai 692954, Russia

Received 2022 Apr. 05, Revised 2022 May 01

Abstract

We studied Romanov V48, which had been considered as a possible polar below the period minimum (orbital period of 0.0420991 d). We analyzed the publicly available Zwicky Transient Facility data and found that this object is an intermediate polar with an orbital period of 0.102312 d (in the period gap) and a spin period of 0.0420991 d. The amplitude of the spin variation was very large (0.6 mag) and the profile has been confirmed to vary with the beat period of 0.071534 d. The ratio between the spin and orbital periods was large and the system resembles the intermediate polar DW Cnc below the period gap. Infrared emission from Romanov V48, however, could not be explained by radiation from the secondary. The infrared excess and the shape of the spectral energy distribution resembled those of polars, suggesting that the emission mechanism in Romanov V48 is similar to those of polars. Romanov V48 may be an intermediate object between intermediate polars and polars.

The object Gaia EDR3 2236896418906579072 at $20^{\rm h}\ 11^{\rm m}\ 16\overset{\rm s}{.}825$, $+60^\circ\ 04'\ 28\overset{''}{.}04$ (J2000.0) has BP=17.407, RP=17.000 and a parallax ϖ=0.693(65) mas (Gaia Collaboration et al. 2021). The variability of this object was detected by the Asteroid Terrestrial-impact Last Alert System (ATLAS: Tonry et al. 2018) as ATO J302.8201+60.0744 with a classification of "dubious" (unspecified variable stars not classified into the 12 categories including pulsating, eclipsing or other representative variables) (Heinze et al. 2018). Heinze et al. (2018) gave a period of 0.081328 d (by Lomb-Scargle method: Scargle 1982). This object has an X-ray counterpart of 1RXS J201117.9+600421. The Zwicky Transient Facility (ZTF: Masci et al. 2019) also detected the variability of this object and listed it as a candidate variable star with a range of 16.783–18.188 mag and a possible period of 0.0404 d (Ofek et al. 2020). Using Gaia DR2 (Gaia Collaboration et al. 2018), Mowlavi et al. (2021) selected candidate variable stars and listed this object as a short time-scale candidate (DR2_STS). The catalog by Mowlavi et al. (2021) was released in 2020 September in arXiv.

One of the authors (Filipp Romanov, hereafter FR) noticed this object when comparing X-ray sources (such as ROSAT sources) and ultraviolet-excess objects (GALEX: Martin et al. 2005) with blue stars on the Aladin Sky Atlas to search for cataclysmic variables (CVs). FR was the first to correctly identify the period of 0.0420991 d using ZTF DR4 and the Pan-STARRS1 (PS1: Chambers et al. 2016) surveys. Sebastián Otero, the chief supervisor of the American Association of Variable Stars (AAVSO) Variable Star Index (VSX: Watson et al. 2006) suggested a classification of a candidate polar (AM:). FR reported these results to the AAVSO VSX with the name of Romanov V48 on 2021 February 23[1]. We hereafter use this designation for this object.

[1] <https://www.aavso.org/vsx/index.php?view=detail.top&oid=2215537>.

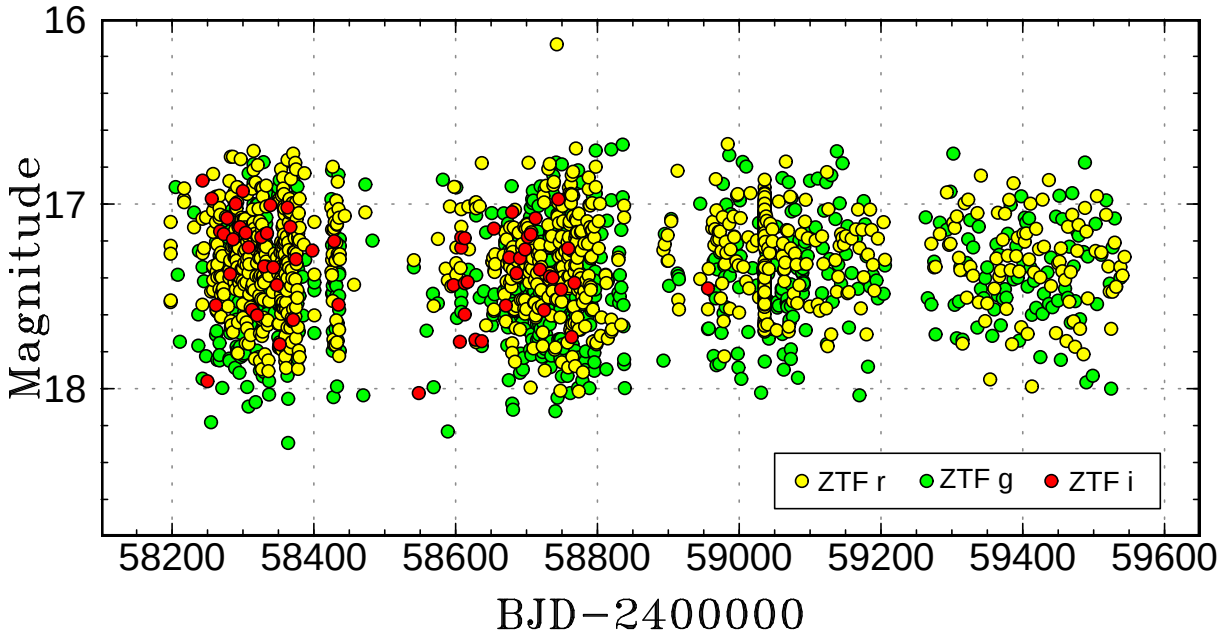

Figure 1: Long-term ZTF light curve of Romanov V48.

Since the period is far shorter than the "period minimum" of CVs (Kolb 1993; Howell et al. 1997; Gänsicke et al. 2009; Knigge 2006; Knigge et al. 2011; Kato 2022), we made a more detailed analysis and tried to clarify the nature of the object. We analyzed the light variation using the ZTF public data[2]. The long-term variation is shown in figure 1. There was no difference between g, r and i light curves and there was no high/low states which are usually seen in many polars. There was one sequence of time-resolved photometry in the ZTF data (figure 2). The presence of flickering is characteristic to a CV. The box-shaped, large-amplitude (0.7 mag) orbital variation is similar to that of a polar and does not resemble the orbital variation of a dwarf nova. A phase dispersion minimization (PDM: Stellingwerf 1978) analysis of the ZTF data confirmed the period detected by FR (figure 3). The period was determined to be 0.04209909(2) d, whose error was estimated by the methods of Fernie (1989) and Kato et al. (2010). The light curve phased with this period is shown in figure 4. There is no difference in the profile between the three ZTF bands and the colors were almost zero. The presence of two maxima of different amplitudes within one phase excludes the possibility of the double period being the true one.

Baran et al. (2021) reported on a search for pulsating subdwarf B star using the Transiting Exoplanet Survey Satellite (TESS) full frame images and Romanov V48 was included in their sample (under the name of 2236896418906579072). Baran et al. (2021) included this object among 30 sdBV candidates that were not spectroscopically classified (in their table 3 and figure 7). Although the power spectrum by Baran et al. (2021) detected the period we determined at 275μHz, Baran et al. (2021) did not mention it. The signal at 113μHz in Baran et al. (2021) is indeed present in the ZTF data. The period has been determined to be 0.1023116(4) d (figure 5). The amplitude of the 0.1023116-d period was 0.4 mag, smaller than that of the 0.04209909-d period. We could not detect a signal around 12μHz (=0.96 d) in the ZTF data. We refer to the 0.04209909-d period as P_1 0.1023116-d period one as P_2. The maxima can be expressed as

$$\text{Max } (P_1) \text{ (BJD)} = 2458718.664(1) + 0.04209909(2)E \quad (1)$$

and

$$\text{Max } (P_2) \text{ (BJD)} = 2458718.657(1) + 0.1023116(4)E. \quad (2)$$

The presence of two periods P_1 and P_2 suggests an intermediate polar (IP). In this interpretation, P_2 is the orbital period ($P_{\rm orb}$) and it is in the period gap. In this case, we can expect a signal at the beat period between

[2]The ZTF data can be obtained from IRSA <https://irsa.ipac.caltech.edu/Missions/ztf.html> using the interface <https://irsa.ipac.caltech.edu/docs/program_interface/ztf_api.html> or using a wrapper of the above IRSA API <https://github.com/MickaelRigault/ztfquery>.

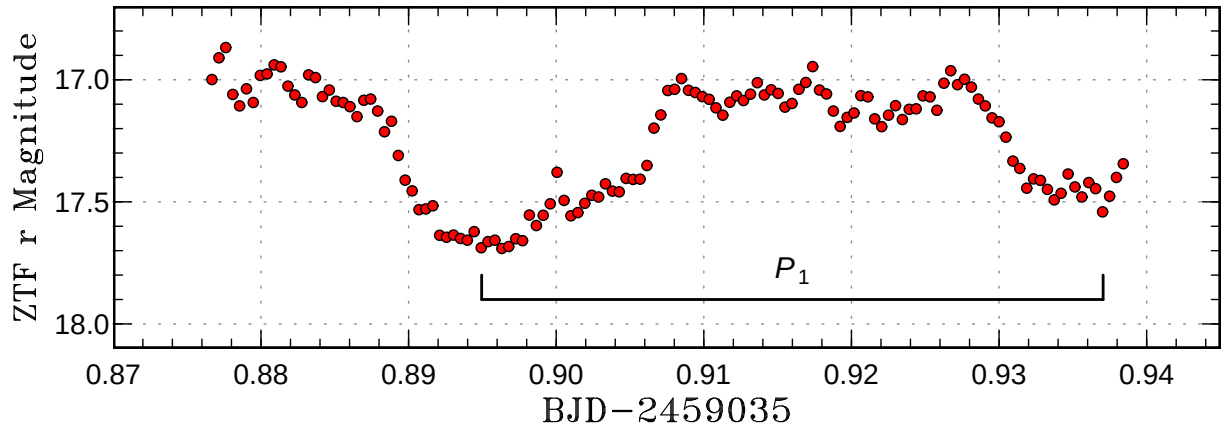

Figure 2: ZTF light curve of Romanov V48 on 2020 July 5. Flickering and large-amplitude orbital variation are present.

P_1 (spin period) and P_2. This is indeed the case and a period P_3=0.0715335(2) d was detected (figure 6). This signal was not apparent in the figure of Baran et al. (2021). The ephemeris is

$$\text{Max } (P_3) \text{ (BJD)} = 2458718.668(1) + 0.0715335(2)E. \quad (3)$$

This period reflects the period in which the beamed light from the magnetic poles on the white dwarf sweeps the surface of the secondary. The existence of this period is a strong support to the IP interpretation. We could detect systematic variations of pulse profiles depending on the beat phase (figure 7). These variations reflect the geometry of the magnetic poles against the accretion stream from the secondary.

IPs inside or below the period gap are relatively rare and well-established ones having $P_{\rm orb}$ shorter than Romanov V48 are: V455 And (Araujo-Betancor et al. 2005), HT Cam (Tovmassian et al. 1998; Kemp et al. 2002), V1025 Cen (Buckley et al. 1998; Hellier et al. 2002), DW Cnc (Patterson et al. 2004), EX Hya (Sterken et al. 1983; Jablonski and Busko 1985), CC Scl (Woudt et al. 2012; Kato et al. 2015), AX J1853.3−0128, IGR J18173−2509 (Thorstensen and Halpern 2013) and Swift J0503.7−2819 (Halpern and Thorstensen 2015). According to Koji Mukai's "The Intermediate Polars" page[3], only one IP was plotted on his diagram [V515 And: (Butters et al. 2008; Kozhevnikov 2012); $P_{\rm orb}$ has not been directly determined]. Many IPs follow the relation between spin period ($P_{\rm spin}$) and $P_{\rm orb}$ on the line $P_{\rm spin}/P_{\rm orb} \simeq 0.1$ or less (Patterson 1994). Among the objects listed, V1025 Cen, DW Cnc, EX Hya and IGR J18173−2509 are the exceptions. Norton et al. (2008) explained a larger fraction of IPs having large $P_{\rm spin}/P_{\rm orb}$ in short-$P_{\rm orb}$ systems considering the evolution and the spin equilibrium. Romanov V48 appears to be most similar to DW Cnc although Romanov V48 is in the period gap and has larger amplitudes of spin pluses. The absolute magnitude of Romanov V48 (M_V=+6.5) is the brightest among these objects except IGR J18173−2509 whose distance is unknown.

Romanov V48 has an excess infrared emission in 2MASS J, H (Cutri et al. 2003) and the Wide-field Infrared Survey Explorer (WISE: Wright et al. 2010) W1 and W2 bands (the object was below the detection limit in 2MASS $K_{\rm s}$, WISE W3 and W4). Even a donor with an evolved core [such as in QZ Ser (Thorstensen et al. 2002)] cannot explain the spectral energy distribution (SED) in the infrared, while the infrared SED of DW Cnc is on the Rayleigh-Jeans tail of a hot object (figure 8). The infrared excess resembles that of a polar as shown in the figure. IPHAS J052832.69+283837.6 was chosen as an example of a polar (Borisov et al. 2016) [see e.g. Harrison and Campbell (2015) for infrared SEDs of other polars]. The infrared excess in Romanov V48 may suggest that the emission mechanism in this system is similar to those in polars. The large amplitudes of the spin pulses may also suggest a magnetic field stronger than the majority of IPs. Having a large $P_{\rm spin}/P_{\rm orb}$, Romanov V48 may be an intermediate object between IPs and polars. Polarimetric, X-ray and spectroscopic observations are encouraged.

[3] <https://asd.gsfc.nasa.gov/Koji.Mukai/iphome/iphome.html>.

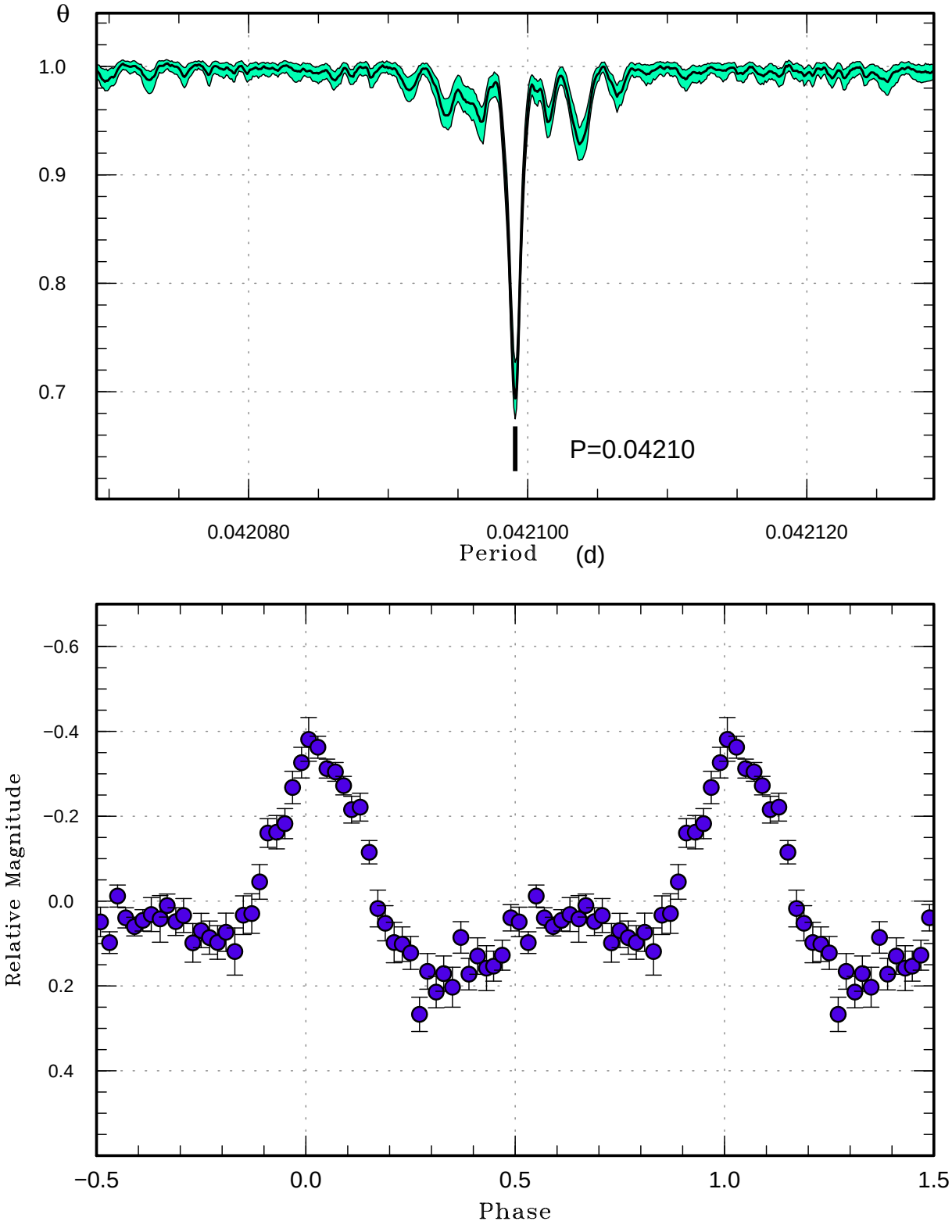

Figure 3: PDM analysis of Romanov V48 using the ZTF data of the shorter period (P_1) = spin period. (Upper): PDM analysis. The bootstrap result using randomly contain 50% of observations is shown as a form of 90% confidence intervals in the resultant θ statistics. (Lower): mean profile. 1σ error bars are shown.

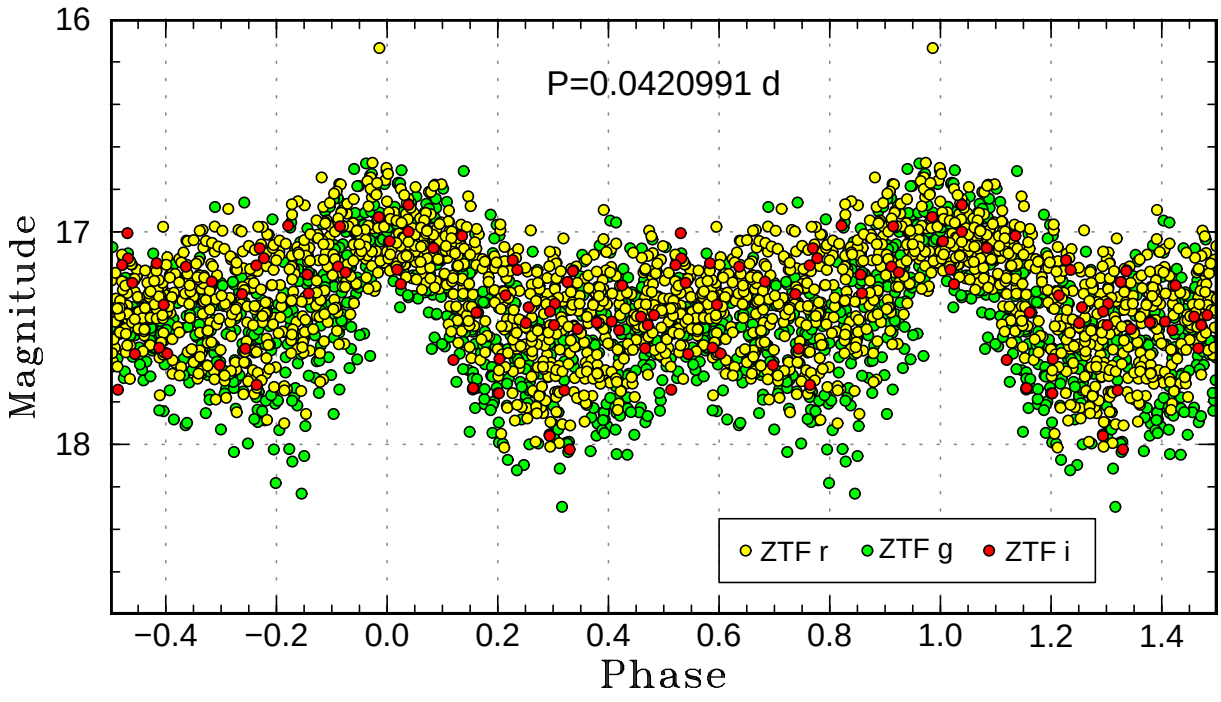

Figure 4: The light curve of Romanov V48 using the ZTF data folded by P_1. The zero epoch was chosen as BJD 2458718.664.

Acknowledgements

This work was supported by JSPS KAKENHI Grant Number 21K03616. The author is grateful to the ZTF team for making their data available to the public. We are grateful to Naoto Kojiguchi for helping downloading the ZTF data. This research has made use of the AAVSO Variable Star Index and NASA's Astrophysics Data System.

Based on observations obtained with the Samuel Oschin 48-inch Telescope at the Palomar Observatory as part of the Zwicky Transient Facility project. ZTF is supported by the National Science Foundation under Grant No. AST-1440341 and a collaboration including Caltech, IPAC, the Weizmann Institute for Science, the Oskar Klein Center at Stockholm University, the University of Maryland, the University of Washington, Deutsches Elektronen-Synchrotron and Humboldt University, Los Alamos National Laboratories, the TANGO Consortium of Taiwan, the University of Wisconsin at Milwaukee, and Lawrence Berkeley National Laboratories. Operations are conducted by COO, IPAC, and UW.

The ztfquery code was funded by the European Research Council (ERC) under the European Union's Horizon 2020 research and innovation programme (grant agreement n°759194 – USNAC, PI: Rigault).

This publication makes use of data products from the Wide-field Infrared Survey Explorer, which is a joint project of the University of California, Los Angeles, and the Jet Propulsion Laboratory/California Institute of Technology, funded by the National Aeronautics and Space Administration.

This publication makes use of data products from the Two Micron All Sky Survey, which is a joint project of the University of Massachusetts and the Infrared Processing and Analysis Center/California Institute of Technology, funded by the National Aeronautics and Space Administration and the National Science Foundation.

List of objects in this paper

V455 And, V515 And, HT Cam, V1025 Cen, DW Cnc, EX Hya, CC Scl, QZ Ser, 1RXS J201117.9+600421, ATO J302.8201+60.0744, AX J1853.3−0128. Gaia EDR3 2236896418906579072, IGR J18173−2509, IPHAS J052832.69+283837.6, Romanov V48, Swift J0503.7−2819

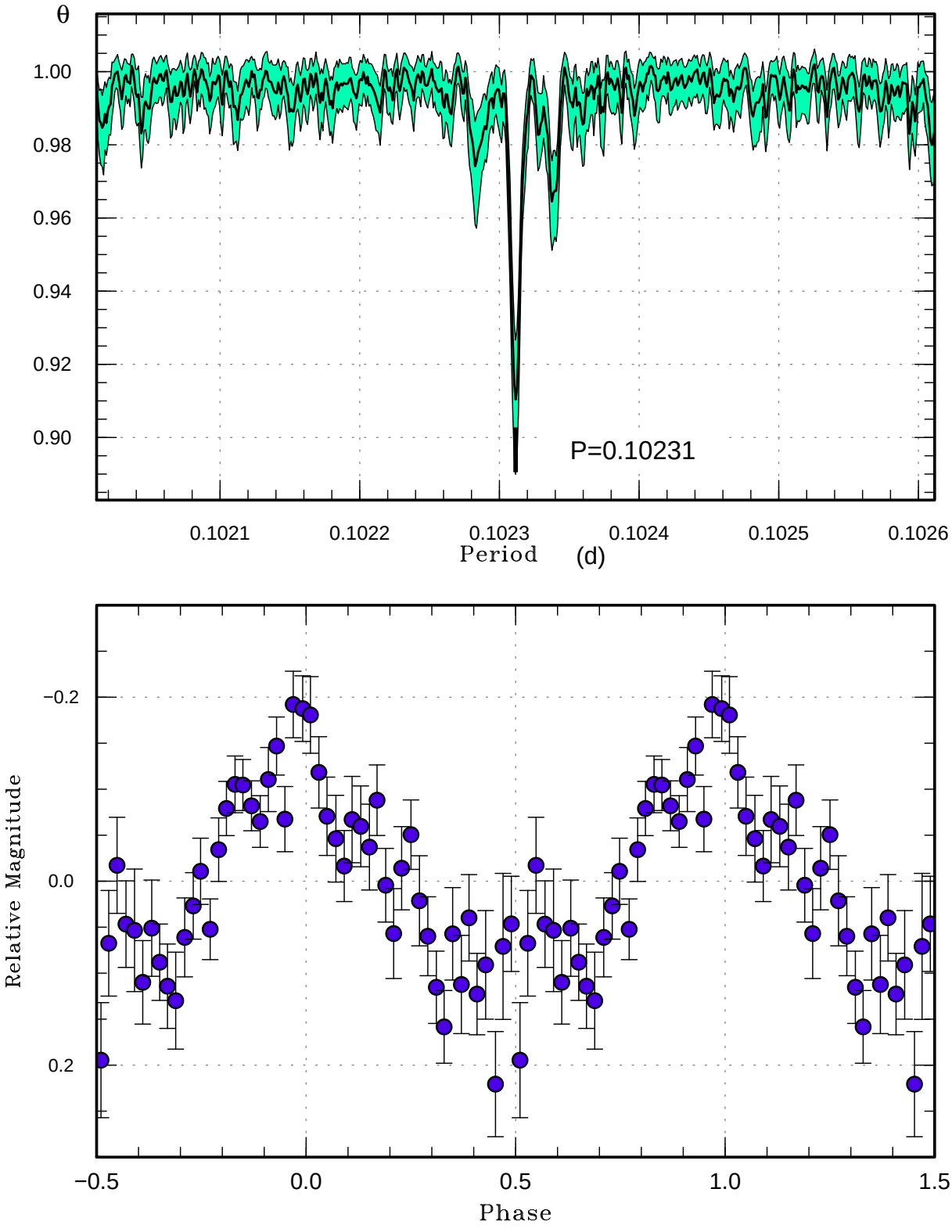

Figure 5: PDM analysis of the longer period (P_2) = orbital period of Romanov V48 using the ZTF data. (Upper): PDM analysis. (Lower): mean profile.

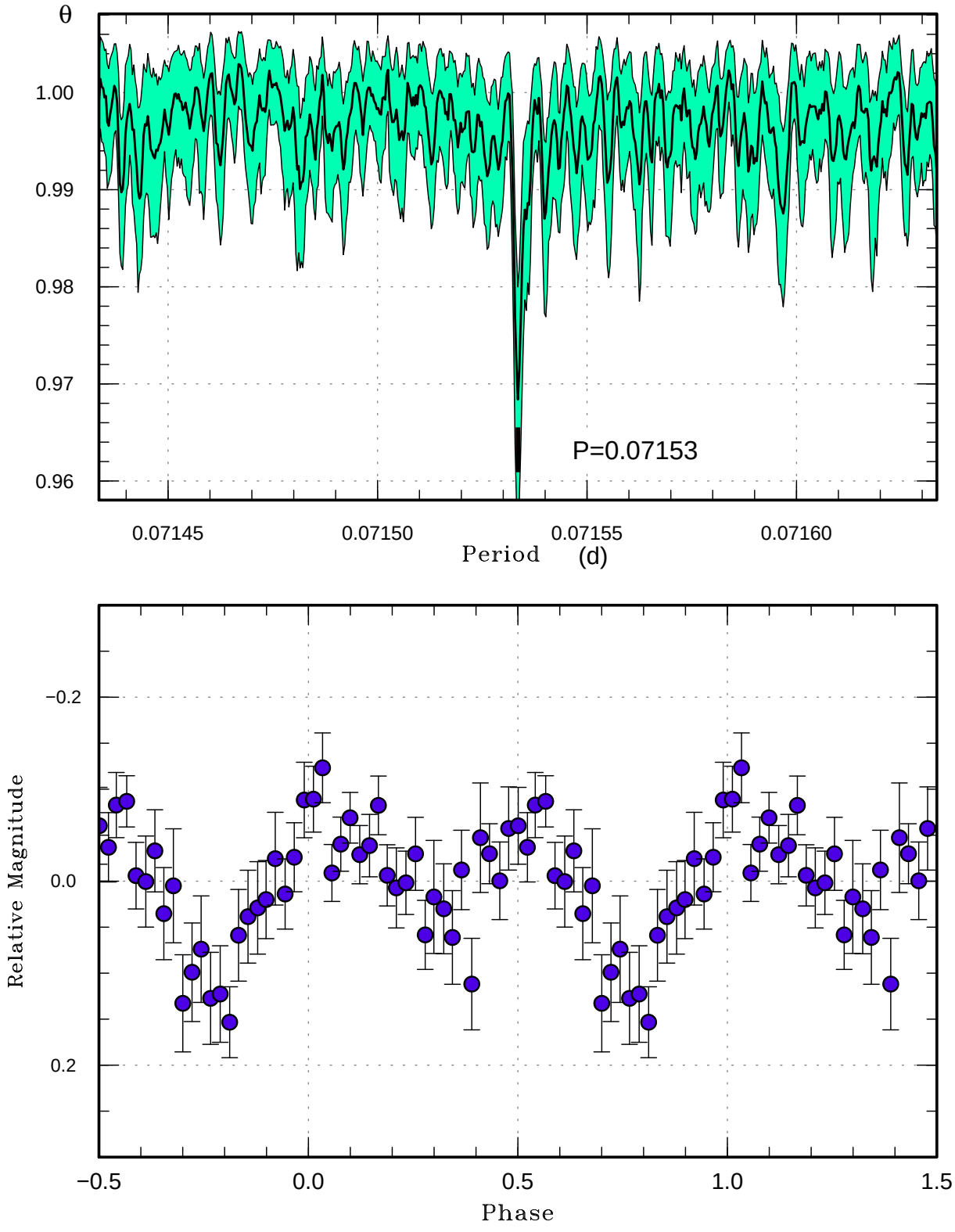

Figure 6: PDM analysis of the beat period (P_3) of Romanov V48 using the ZTF data. (Upper): PDM analysis. (Lower): mean profile.

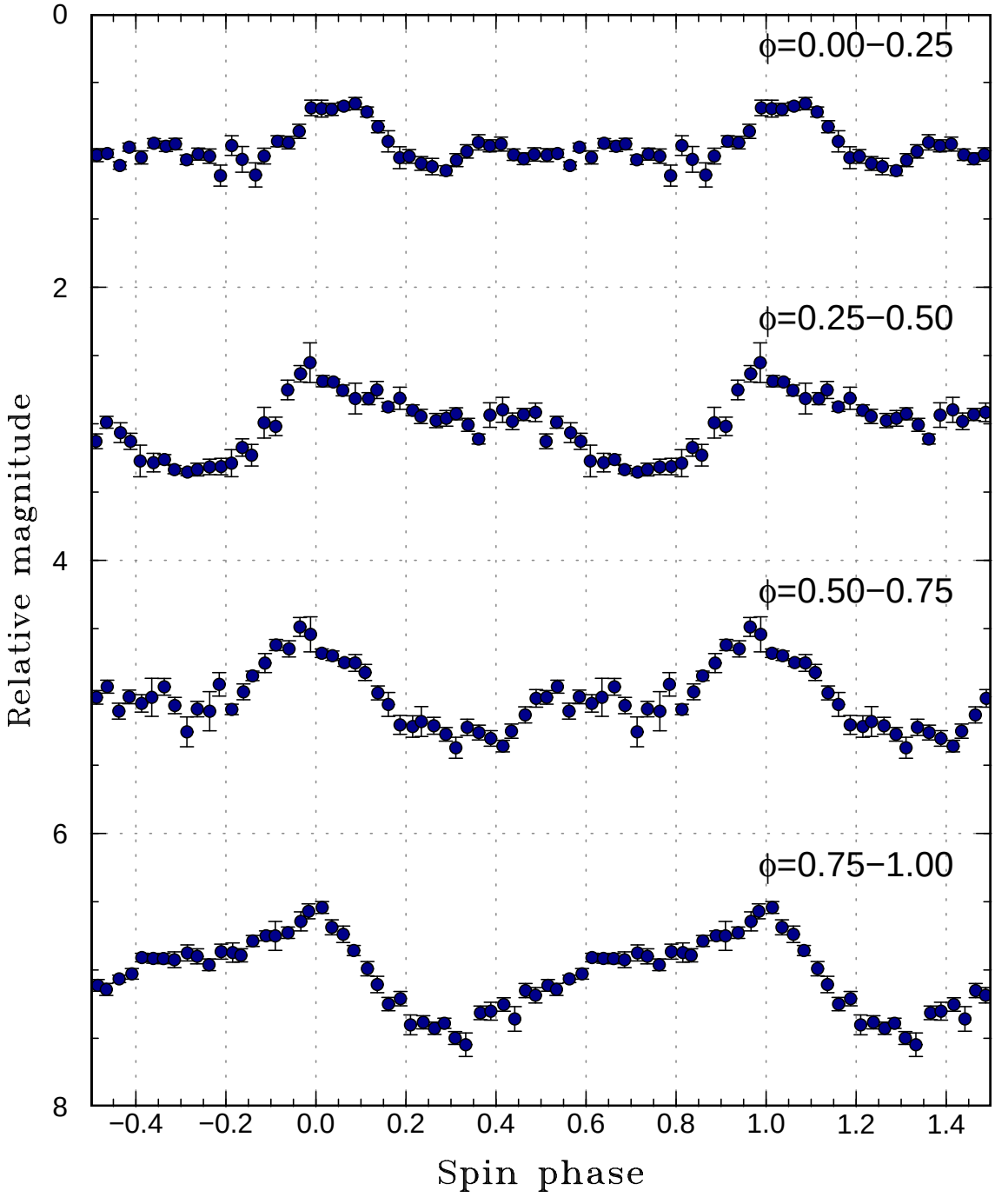

Figure 7: Variation of pulse profiles of Romanov V48 depending on the beat phase (ϕ). The beat phases ϕ were determined using the equation (3). The pulse phases were determined using the equation (1). All bands of the ZTF data were combined.

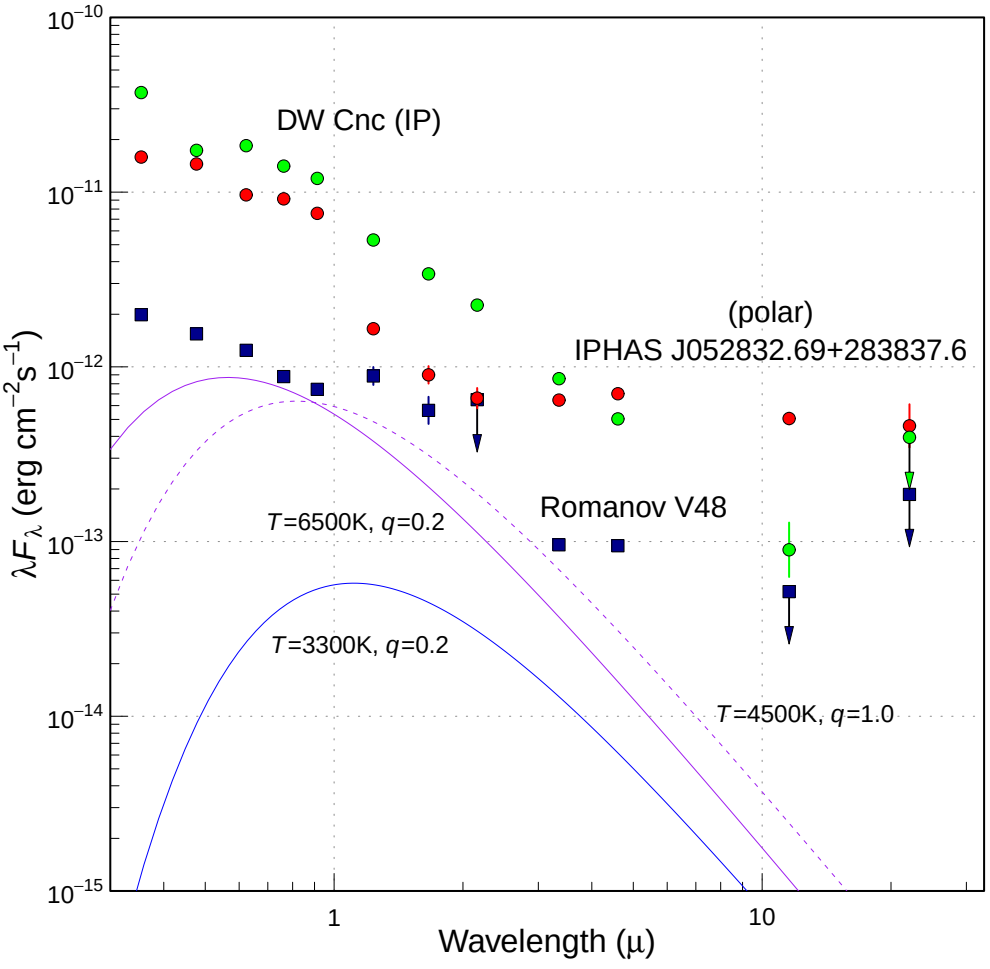

Figure 8: The spectral energy distribution (SED) of Romanov V48 (filled squares). The figure is based on SDSS (York et al. 2000; Ahumada et al. 2020) u',g',r',i',z' magnitudes, 2MASS J, H, $K_{\rm s}$ magnitudes and WISE W1–W4 magnitudes. Zero-point calibrations of the 2MASS magnitudes used Cohen et al. (2003). The short-$P_{\rm orb}$ intermediate polar DW Cnc (green circles) and the short-$P_{\rm orb}$ polar IPHAS J052832.69+283837.6 (red circles) are shown for a comparison. The arrows represent upper limits. The error bars represent 1σ errors arising from photometric errors only. 1σ errors arising from the uncertainty in the distance of Romanov V48 are 0.20 mag. The curves represent the expected black-body radiation for the secondary filling the Roche lobe of a binary with a period of 0.10231 d at the distance of Romanov V48. Three combinations of the mass ratios (q) and temperatures are shown as a typical M-type star and extreme limits. Any donor filling the Roche lobe cannot explain the infrared SED of Romanov V48.

References

Ahumada, R. et al. (2020) The 16th Data Release of the Sloan Digital Sky Surveys: First release from the APOGEE-2 Southern Survey and full release of eBOSS spectra. *ApJS* **249**, 3

Araujo-Betancor, S. et al. (2005) HS 2331+3905: The cataclysmic variable that has it all. *A&A* **430**, 629

Baran, A. S., Sahoo, S. K., Sanjayan, S., & Ostrowski, J. (2021) A search for variable subdwarf B stars in *TESS* full frame images – II. Variable objects in the northern ecliptic hemisphere. *MNRAS* **503**, 3828

Borisov, N. V., Gabdeev, M. M., & Afanasiev, V. L. (2016) Photopolarimetric observations of the sample of polar candidates. *Astrophys. Bull.* **71**, 95

Buckley, D. A. H., Cropper, M., Ramsay, G., & Wickramasinghe, D. T. (1998) The new intermediate polar RX J1238−38: a system below the period gap? *MNRAS* **299**, 83

Butters, O. W., Norton, A. J., Hakala, P., Mukai, K., & Barlow, E. J. (2008) RXTE determination of the intermediate polar status of XSS J00564+4548, IGR J17195−4100, and XSS J12270−4859. *A&A* **487**, 271

Chambers, K. C. et al. (2016) The Pan-STARRS1 surveys. *arXiv e-prints* **arXiv:1612.05560**

Cohen, M., Wheaton, W. A., & Megeath, S. T. (2003) Spectral irradiance calibration in the Infrared. XIV. The absolute calibration of 2MASS. *AJ* **126**, 1090

Cutri, R. M. et al. (2003) 2MASS All Sky Catalog of point sources (NASA/IPAC Infrared Science Archive)

Fernie, J. D. (1989) Uncertainties in period determinations. *PASP* **101**, 225

Gaia Collaboration et al. (2018) Gaia Data Release 2. Summary of the contents and survey properties. *A&A* **616**, A1

Gaia Collaboration et al. (2021) Gaia Early Data Release 3. Summary of the contents and survey properties. *A&A* **649**, A1

Gänsicke, B. T. et al. (2009) SDSS unveils a population of intrinsically faint cataclysmic variables at the minimum orbital period. *MNRAS* **397**, 2170

Halpern, J. P., & Thorstensen, J. R. (2015) Optical studies of 13 hard X-ray selected cataclysmic binaries from the Swift-BAT survey. *AJ* **150**, 170

Harrison, T. E., & Campbell, R. K. (2015) The WISE light curves of polars. *ApJS* **219**, 32

Heinze, A. N. et al. (2018) A first catalog of variable stars measured by the Asteroid Terrestrial-impact Last Alert System (ATLAS). *AJ* **156**, 241

Hellier, C., Wynn, G. A., & Buckley, D. A. H. (2002) On the accretion mode of the intermediate polar V1025 Centauri. *MNRAS* **333**, 84

Howell, S. B., Rappaport, S., & Politano, M. (1997) On the existence of low-luminosity cataclysmic variables beyond the orbital period minimum. *MNRAS* **287**, 929

Jablonski, F., & Busko, I. C. (1985) EX Hya – the slowest DQ Her star? *MNRAS* **214**, 219

Kato, T., Hambsch, F.-J., Oksanen, A., Starr, P., & Henden, A. (2015) CC Sculptoris: Eclipsing SU UMa-type intermediate polar. *PASJ* **67**, 3

Kato, T. (2022) Evolution of short-period cataclysmic variables: implications from eclipse modeling and stage a superhump method (with New Year's gift). *VSOLJ Variable Star Bull.* **89**, (arXiv:2201.02945)

Kato, T. et al. (2010) Survey of Period Variations of Superhumps in SU UMa-Type Dwarf Novae. II. The Second Year (2009-2010). *PASJ* **62**, 1525

Kemp, J., Patterson, J., Thorstensen, J. R., Fried, R. E., Skillman, D. R., & Billings, G. (2002) Rapid oscillations in cataclysmic variables. XV. HT Camelopardalis (=RX J0757.0+6306). *PASP* **114**, 623

Knigge, C. (2006) The donor stars of cataclysmic variables. *MNRAS* **373**, 484

Knigge, C., Baraffe, I., & Patterson, J. (2011) The evolution of cataclysmic variables as revealed by their donor stars. *ApJS* **194**, 28

Kolb, U. (1993) A model for the intrinsic population of cataclysmic variables. *A&A* **271**, 149

Kozhevnikov, V. P. (2012) An extensive photometric study of the recently discovered intermediate polar V515 And (XSS J00564+4548). *MNRAS* **422**, 1518

Martin, D. C. et al. (2005) The Galaxy Evolution Explorer: A space ultraviolet survey mission. *ApJ* **619**, L1

Masci, F.-J. et al. (2019) The Zwicky Transient Facility: Data processing, products, and archive. *PASP* **131**, 018003

Mowlavi, N. et al. (2021) Large-amplitude variables in Gaia Data Release 2. Multi-band variability characterization. *A&A* **648**, A44

Norton, A. J., Butters, O. W., Parker, T. L., & Wynn, G. A. (2008) The accretion flows and evolution of magnetic cataclysmic variables. *ApJ* **672**, 524

Ofek, E. O., Soumagnac, M., Nir, G., Gal-Yam, A., Nugent, P., Masci, F., & Kulkarni, S. R. (2020) A catalogue of over 10 million variable source candidates in ZTF Data Release 1. *MNRAS* **499**, 5782

Patterson, J. et al. (2004) Rapid oscillations in cataclysmic variables. XVI. DW Cancri. *PASP* **116**, 516

Patterson, J. (1994) The DQ Herculis stars. *PASP* **106**, 209

Scargle, J. D. (1982) Studies in astronomical time series analysis. II – statistical aspects of spectral analysis of unevenly spaced data. *ApJ* **263**, 835

Stellingwerf, R. F. (1978) Period determination using phase dispersion minimization. *ApJ* **224**, 953

Sterken, C., Vogt, N., Freeth, R., Kennedy, H. D., Marino, B. F., Page, A. A., & Walker, W. S. G. (1983) EX Hydrae – a coordinated campaign of photoelectric photometry from four observatories. *A&A* **118**, 325

Thorstensen, J. R., Fenton, W. H., Patterson, J. O., Kemp, J., Halpern, J., & Baraffe, I. (2002) QZ Serpentis: A dwarf nova with a 2-hour orbital period and an anomalously hot, bright secondary star. *PASP* **114**, 1117

Thorstensen, J. R., & Halpern, J. (2013) Optical and X-ray studies of 10 X-ray-selected cataclysmic binaries. *AJ* **146**, 107

Tonry, J. L. et al. (2018) ATLAS: A High-cadence All-sky Survey System. *PASP* **130**, 064505

Tovmassian, G. H. et al. (1998) A new cataclysmic variable RX J0757.0+6306: candidate for the shortest period intermediate polar. *A&A* **335**, 227

Watson, C. L., Henden, A. A., & Price, A. (2006) The International Variable Star Index (VSX). *Society for Astronom. Sciences Ann. Symp.* **25**, 47

Woudt, P. A. et al. (2012) CC Sculptoris: A superhumping intermediate polar. *MNRAS* **427**, 1004

Wright, E. L. et al. (2010) The Wide-field Infrared Survey Explorer (WISE): Mission description and initial on-orbit performance. *AJ* **140**, 1868

York, D. G. et al. (2000) The Sloan Digital Sky Survey: Technical summary. *AJ* **120**, 1579

VSOLJ
c/o Keiichi Saijo National Science Museum, Ueno-Park, Tokyo Japan

Editor Seiichiro Kiyota
e-mail: skiyotax@gmail.com